

Deformation of CoTi polycrystals

T. TAKASUGI, O. IZUMI

Institute for Materials Research, Tohoku University, Sendai, Japan

Deformation behaviour of polycrystalline B2-type CoTi intermetallic compounds was investigated in relation to testing temperature (77 to 1073 K), alloy composition (50 to 48 at.% Ti) and strain rate (4.2×10^{-4} to $4.2 \times 10^{-3} \text{ sec}^{-1}$). Four distinct temperature regions were distinguished. A low-temperature region where the yield stress rapidly decreased with temperature; an intermediate temperature region where the yield stress increased with temperature, accompanied by very high strain-hardening rate, serration on the stress-strain curves and kink deformation; a high temperature region where the yield stress again rapidly decreased with temperature, and a very high temperature region where the yield stress slowly decreased with temperature. Deviation from stoichiometry resulted in increased yield stresses over whole temperature regions. Positive strain-rate dependence of the yield stress was regarded in the two higher temperature regions. Slip traces were observed at all temperatures. Possible explanations are given in comparison with other B2-type intermetallic compounds.

1. Introduction

There are many B2(L2₀) (i.e. CsCl)-type intermetallic compounds which remain ordered up to the melting point, e.g. the aluminides of NiAl, FeAl and CoAl, the titanides of NiTi, FeTi and CoTi, AgMg and AuZn. In addition, CuZn and FeCo are the same kind of alloys which undergo the order-disorder transformation below the melting temperature. The mechanical behaviour has been reported for the polycrystals as well as the single crystals of these alloys, except for the titanides (see review articles [1, 2]). The polycrystals of investigated B2-type intermetallic compounds tend to be brittle and reveal a significant temperature dependence of the flow stress below room temperature. Beyond room temperature to about $0.45 T_m$, the ductility remains low, but the yield stress decreases slowly with temperature. Above $0.45 T_m$, the flow stress decreases rapidly, accompanied with considerable ductility.

The single crystals of investigated B2-type intermetallic compounds show somewhat similar temperature dependence of yield stress to that in the polycrystals and also appear to be rather ductile at room temperature and above. However, the flow properties, like the slip system, are very different, depending on material, temperature and crystal orientation. It has been generally known that the slip direction in B2-type compounds is either $\langle 001 \rangle$ or $\langle 111 \rangle$, and the $\langle 001 \rangle$ -type slip occurs in strongly ordered compounds with high ordering energy and the $\langle 111 \rangle$ -type slip in those with relatively low ordering energy. Also, it has been shown that the transition in the slip direction from $\langle 111 \rangle$ to $\langle 001 \rangle$ occurs at 0.4 to $0.5 T_m$ (T_m is the melting temperature) with increasing temperature, e.g. in FeAl [3, 4] and AgMg [5, 6]. At such transition temperatures, stressing along the (100) orientation tends to prefer $\langle 111 \rangle$ -type slip and stressing along the (111) orientation prefers $\langle 001 \rangle$ -

type slip. This has been interpreted as the difference in the critical resolved shear stress (c.r.s.s.) between the two types of slip. However, the mechanism responsible for both types of slip, their transition and noticeable compositional effect on the deformation, have not been clarified.

The mechanical behaviour of B2-type CoTi, which is categorized as Berthollide-type compound with high ordering energy, has not been reported so far. The melting point of this alloy is at approximately 1600 K and its solid solution ranges from 50 at.% Co to 55 at.% Co as shown in Fig. 1 [7]. In this work, the results of compression tests on the polycrystalline CoTi compound are presented. The mechanical properties are characterized by the yield stress and the plastic flow behaviour up to a few per cent. The temperature dependence and strain-rate effect as the environmental factor and the compositional effect as the material factor are investigated for these properties. Thus, we have tried to elucidate the deformation mechanism of B2-type CoTi compound with high ordering energy, in comparison with other B2-type compounds.

2. Experimental details

Three alloys containing 50 at.% Ti, 49.5 at.% Ti and 48 at.% Ti were prepared by nonconsumable arc melting under an argon gas, using cobalt of 99.9 wt % purity and sponge titanium of 99.8 wt % purity. The buttons of about 120 g were homogenized in a vacuum at 1323 K for 2 days, followed by furnace cooling. The compression specimens, approximately $2.5 \times 2.5 \text{ mm}^2$ in cross-section and 6.5 mm long, were cut from the homogenized buttons by wire-slitting and a precise wheel cutter. Here, the specimen axis was taken perpendicular to the axis of the columnar grain structure which is usually developed from bottom to top of the button during solidification. Some of

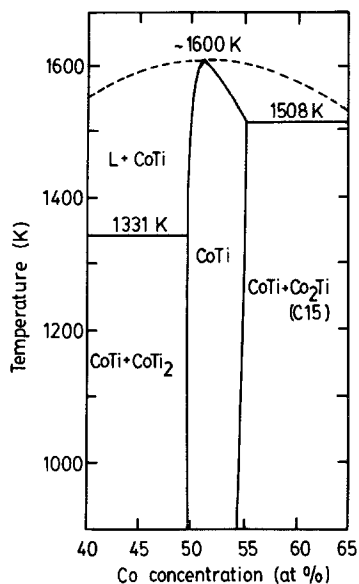


Figure 1 Phase diagram near the equi-atomic composition on the Co-Ti system.

compression specimens were subsequently electrolytically polished in a 20% H_2SO_4 -methanol solution in order to prepare surfaces suitable for the observation of deformation markings.

Compression tests were conducted on an Instron-type machine at initial strain rates of 4.2×10^{-4} and $4.2 \times 10^{-3} \text{ sec}^{-1}$ at temperatures from 77 to 1073 K. These tests at 77 K were performed in liquid nitrogen where the specimens were immersed. The remaining tests were performed under a vacuum of about $1.3 \times 10^{-3} \text{ Pa}$. Specimens were mostly deformed to about a few percent strain and then deformation markings such as slip traces were observed with an optical

microscope using Nomarsky interference contrast. In addition, fractography was observed on the specimens which were fractured by a simple bending test at room temperature.

Specimens for X-ray diffraction were filed; powders consisting of a partial size of 250 mesh were prepared from the above homogenized buttons. X-ray diffraction measurements were carried out on as-crushed powders and fully annealed powders using $CuK\alpha$ radiation. This test was undertaken to examine whether the stress-induced martensite would be introduced by the plastic deformation.

3. Results

3.1. Temperature dependence of yield stress

The temperature dependence of the 0.2% yield stress of CoTi containing 50 at.% Ti, 49.5 at.% Ti and 48 at.% Ti, which was measured at a strain rate of $4.2 \times 10^{-4} \text{ sec}^{-1}$, is shown in Fig. 2; four distinct temperature regions can be distinguished.

(i) Low temperatures ($< 300 \text{ K}$): the yield stress is strongly dependent on the temperature and decreases with increasing temperature.

(ii) Intermediate temperatures (300 to 600/700 K): the yield stress increases with increasing temperature and reaches the peak temperature.

(iii) High temperatures (600/700 to 1000 K): the yield stress is again strongly dependent on the temperature and decreases with increasing temperature.

(iv) Very high temperatures ($> 1000 \text{ K}$): the yield stress is essentially independent of temperature and may be referred to as the athermal stress.

The compositional effect on the temperature-yield stress curves, shows that the lower titanium content

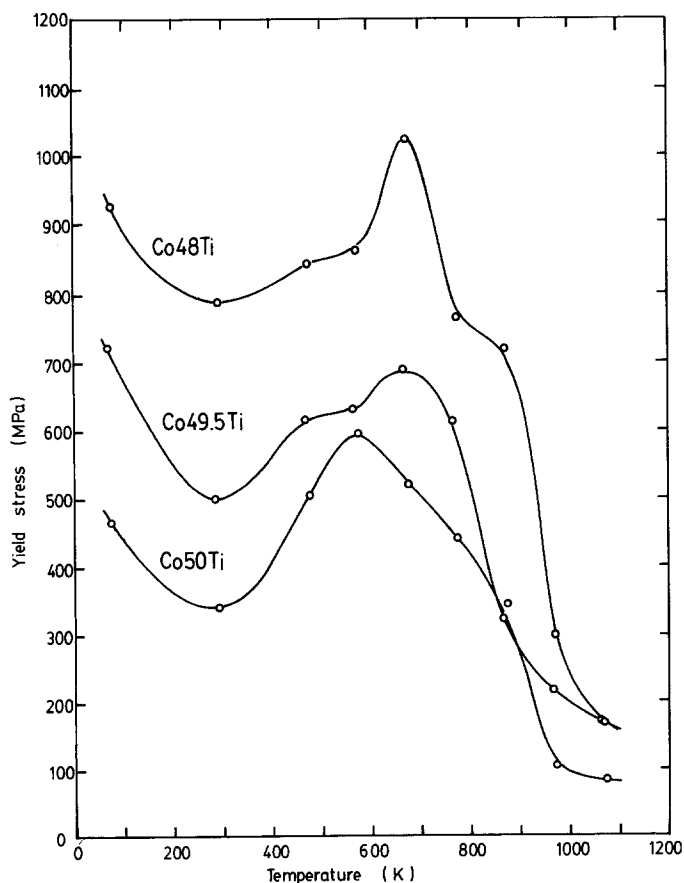


Figure 2 Temperature and composition dependences of the yield stress of CoTi polycrystals, measured at a strain rate of $4.2 \times 10^{-4} \text{ sec}^{-1}$.

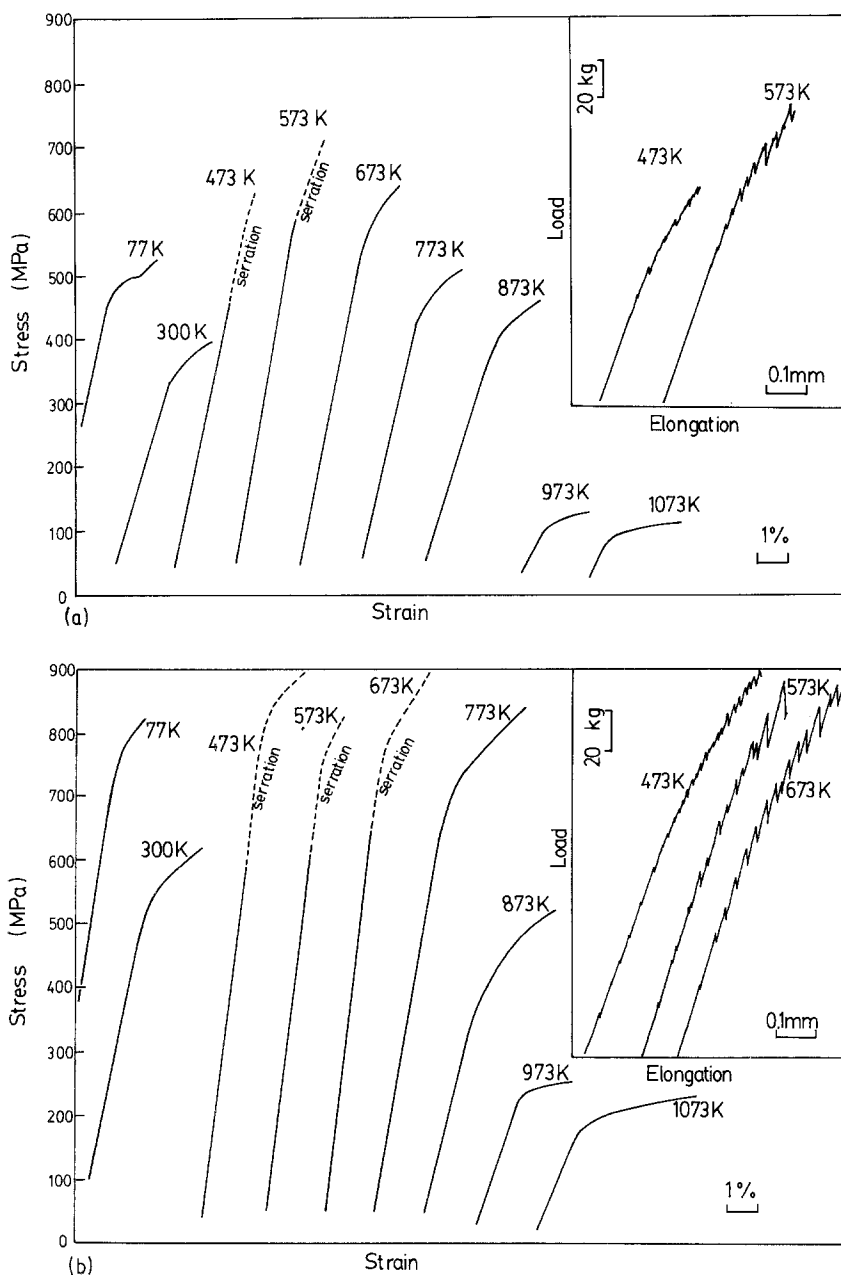


Figure 3 Stress-strain curves of CoTi polycrystals containing (a) 50 at.% Ti, (b) 49.5 at.% Ti and (c) 48 at.% Ti, which were deformed at various temperatures and measured at a strain rate of $4.2 \times 10^{-4} \text{ sec}^{-1}$. Note that the crosses at the ends of the stress-strain curves mark the fracturing of the specimens.

resulted in higher values of yield stress particularly in regions (i), (ii) and (iii). It is also noted that the peak temperature tends to increase as the titanium content decreases.

3.2. Plastic behaviour (Stress-strain curve)

The temperature dependence of the stress-strain curve in CoTi containing 50 at.% Ti, 49.5 at.% Ti and 48 at.% Ti (from which the values of the yield stresses were taken) is shown in Figs 3a, b and c, respectively. The distinctive behaviour can again be seen in each region.

(i) Low temperatures: the flow stress curve, i.e. strain-hardening rate is basically independent of temperature.

(ii) Intermediate temperatures: several anomalous prominent features are seen in this region. The strain-hardening rate is very high. The stress-strain curves are not smooth, but regularly serrated. Correspondingly, audible clicks were heard, accompanying every load drop in the elongation-load curves. This anomalous serration tends to be more significant with

increasing temperature and with increasing plastic strain, as clearly shown in these figures. Also, it is noticed that CoTi containing low titanium content shows more noticeable serrations.

(iii) High temperatures: the strain-hardening rate decreases with increasing temperature.

(iv) Very high temperatures: the steady state flow is apparent, i.e. the stress-strain curves show almost no strain-hardening rate after yielding, suggesting the occurrence of diffusional (creep) flow.

Strain-hardening rate after yielding was also evaluated from the difference in the flow stress levels between 1 and 0.2% plastic strains (i.e. $\Delta\sigma = \sigma_{1\%} - \sigma_{0.2\%}$). Figs 4a, b and c show the temperature-dependence of this strain-hardening rate of CoTi containing 50 at.% Ti, 49.5 at.% Ti and 48 at.% Ti, respectively. $\Delta\sigma$ shows the maximum (peak) approximately at a temperature where the maximum in the yield stress-temperature curve (see Figs 2a, b and c) appeared. Thus, it is strongly suggested that at intermediate temperatures there is a tight correlation between the yield stress and the strain-hardening behaviour.

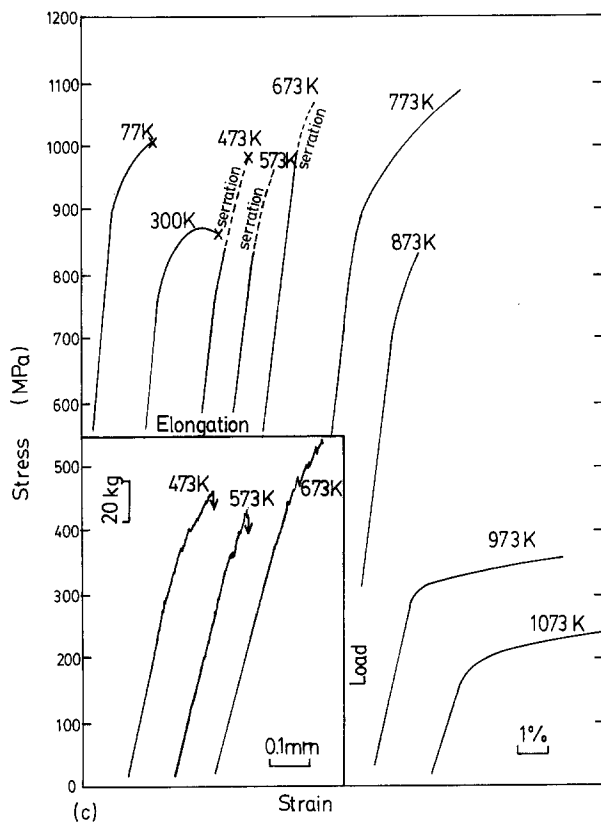


Figure 3 Continued.

3.3. Strain-rate effect

In order to examine the strain-rate effect on the deformation behaviour of CoTi, compression tests were also carried out at a strain rate of $4.2 \times 10^{-3} \text{ sec}^{-1}$, i.e. at a ten-fold increase and then compared with the tests done in the previous section.

Figs 5a, b and c represent the strain-rate effect on the temperature–yield stress relation. Although in temperature regions (i) and (ii) the strain-rate effects are contradictory between the three alloy compositions, in regions (iii) and (iv), i.e. beyond the peak temperature, a positive strain-rate dependence of the yield stress can be seen.

In Figs 4a, b and c the variations of strain-hardening rate with temperature were compared at both strain rates measured; a particular feature is that the peak in the $\Delta\sigma$ –temperature curves became small and thus ambiguous at higher strain rates ($4.2 \times 10^{-3} \text{ sec}^{-1}$).

3.4. Deformation markings

Detailed observations of deformation markings were performed on CoTi containing 49.5 at.% Co, tested at a strain rate of $4.2 \times 10^{-4} \text{ sec}^{-1}$. The results observed at each temperature are shown in Fig. 6. Slip traces were observed at all test temperatures. At low temperatures (for example, region i) the slip traces were somewhat coarse, wavy and band-like, while at high temperatures (for example, region iii) they were fine and straight, as shown in these figures. The most interesting result for the deformation markings was observed in the specimens tested in the intermediate temperature region (ii) where anomalous positive temperature dependence of the yield stress occurred.

Kinks were the distinct deformation mode although they were often mixed with slips. Severe kinking was introduced at the portion near loading contact plane and occasionally preferred to develop along the direction normal to the stress axis, i.e. no “crystallographic” plane. Note in Fig. 6 that the stress axes are shown approximately in the vertical axes in the photographs. No kinks were observed above the peak temperature (regions iii and iv) but a small number of kinks was also observed at low temperatures (region i). Here, it should be noted that the appearance of kinks was associated with serration, high strain-hardening rate and then positive temperature dependence of the yield stress.

The morphological features of the kinks had some characteristics of a martensitic transformation. A stress-induced martensite reaction has been proposed to occur in NiAl polycrystals containing excess nickel [8]. Also, similar markings have been found in NiAl single crystal [9]. However, the fact that the markings which appeared at intermediate temperatures could not be further intensified by testing at low temperatures, for example at 77 K, suggests that they are kinks, but not martensite.

3.5. X-ray diffraction analysis

Figs 7a and b show part of the diffractometer strip-chart records of the well-annealed and as-crushed powders of CoTi containing 49.5 at.% Ti at room temperature with $\text{CuK}\alpha$ radiation. In both specimens, the super-lattice reflection lines were not observable because of a small structure factor of the constituent atoms, $F = f_{\text{Co}} - f_{\text{Ti}}$, relatively rapid scanning rate, and the use of $\text{CuK}\alpha$ radiation. However, detailed measurement of the intensity of the reflection lines by step scanning using $\text{CrK}\alpha$ radiation showed the state of clear ordering in well-annealed CoTi compounds. These are described in a different paper [10]; it was deduced that the excess cobalt atoms introduce the substitutional (anti-) structure in this compound. Here, an emphasized point is that as-crushed specimens containing plastic strain indicated no extra reflection lines. This result suggests that stress- or strain-induced martensitic transformations were not introduced in the specimens deformed at room temperature.

3.6. Fracture behaviour

As shown in the stress–strain curves (Fig. 3), most of the specimens tested sustained the plastic strain up to an intended level. However, premature fracturing occasionally occurred in the specimens containing 48 at.% Co, tested at low temperatures (77 and 300 K). In Fig. 3c, the fracturing is marked by crosses at the ends of the stress–strain curves. By fracturing the specimens were disintegrated into a number of small pieces. Thus, titanium-poor CoTi compound seems to be brittle at low temperatures. Also, simple bending tests were performed at room temperature using the plate-like specimens containing 50 at.% Ti content. The mode of fracture was generally transcrystalline mixed with a small amount of intercrystalline as shown in Fig. 8.

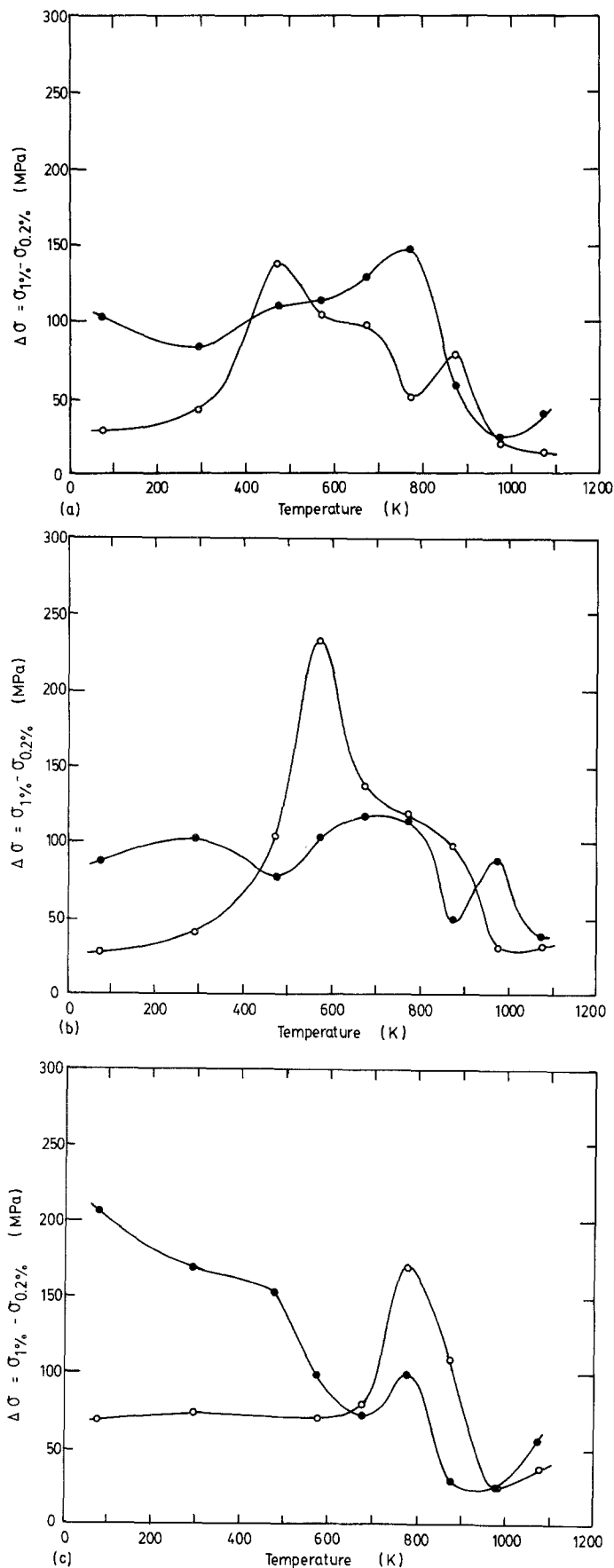


Figure 4 Temperature and strain-rate dependences of the strain-hardening rate of CoTi polycrystals containing (a) 50 at. % Ti, (b) 49.5 at. % Ti and (c) 48 at. % Ti. Note that the strain-hardening rate was evaluated by the difference in the flow stress levels between 1 and 0.2% plastic strains. (○) $\dot{\epsilon} = 4.2 \times 10^{-4} \text{ sec}^{-1}$, (●) $\dot{\epsilon} = 4.2 \times 10^{-3} \text{ sec}^{-1}$.

4. Discussion

Measurements over a wide temperature range demonstrate clearly that CoTi exhibits four stages of temperature dependence of the yield stress, basically similar to those in NiAl [11, 12], AgMg [5, 6, 13], FeAl [3, 4] and AuZn [14] although the last stage has not been reported in previous work.

For region (i) of the single crystals of AgMg [15] and AuZn [16], flow stress has been suggested to be controlled by the Peierls double kink mechanism which has been widely applied to the other bcc metals. Although further work is required, a similar deformation mechanism may be applicable to the present CoTi compound.

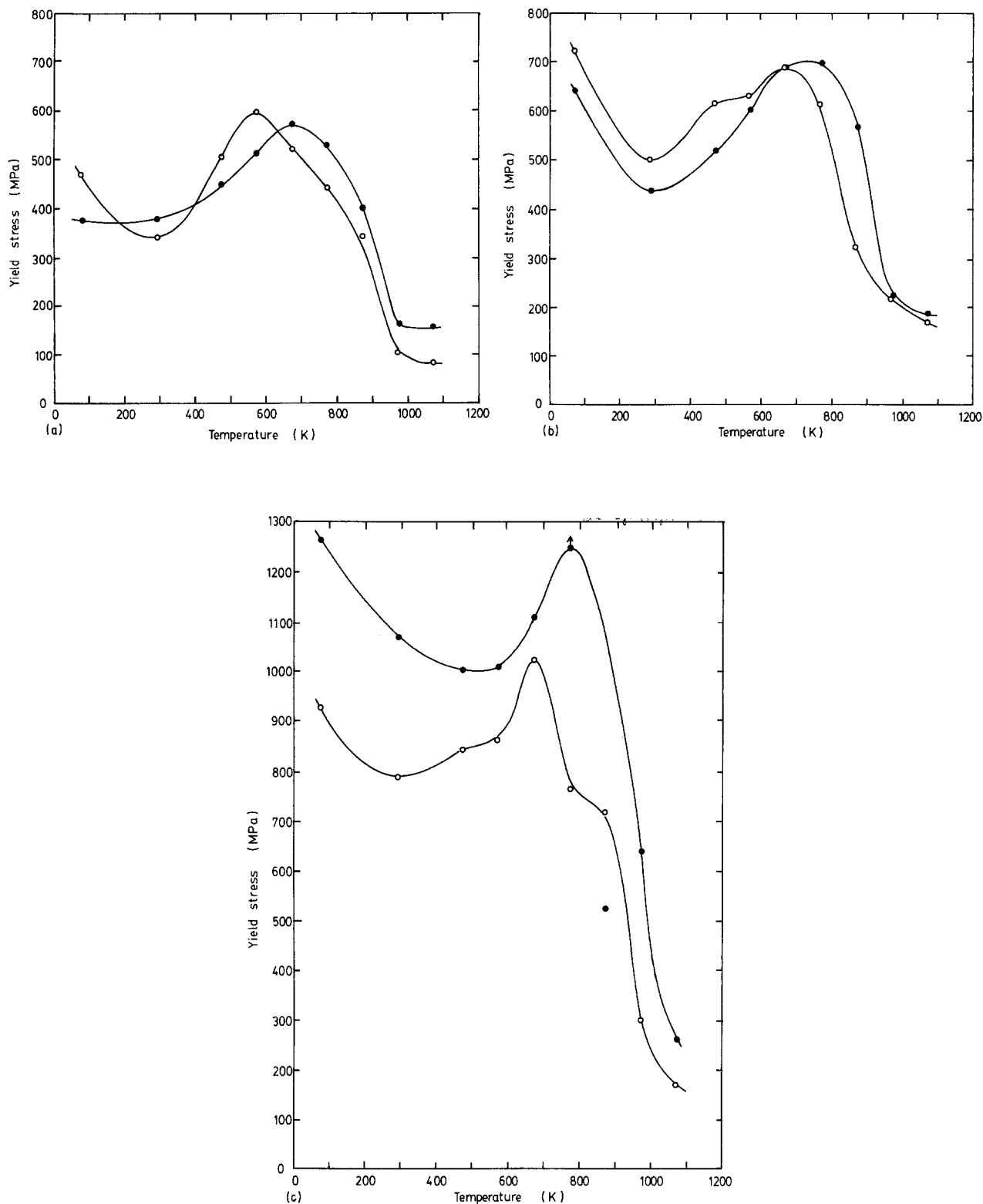


Figure 5 Temperature and strain-rate dependences of the yield stress of CoTi polycrystals containing (a) 50 at.% Ti, (b) 49.5 at.% Ti and (c) 48 at.% Ti. (O) $\dot{\epsilon} = 4.2 \times 10^{-4} \text{ sec}^{-1}$, (●) $\dot{\epsilon} = 4.2 \times 10^{-3} \text{ sec}^{-1}$.

The most emphasized feature was found in region (ii) of CoTi compound. CoTi showed an abnormal positive temperature dependence of yield stress, accompanied by serration and a rapid strain-hardening rate on the stress-strain curve, and by kinks. In previously described compounds, the yield stress was mostly insensitive to temperature, or decreased slowly with increasing temperature. However, similar characteristics were found in NiAl single crystals containing 50 at.% Al with [00 1] orientation [12], although the morphology of the serration on the stress-strain

curve was different between NiAl single crystals and the present CoTi compound. The pitch and magnitude of the serrations were much longer and larger in the former material whereas those of the latter material were short and relatively small. Part of this difference may be attributed to the difference in the deformation between the single crystal and the polycrystal.

The first possible explanation for this abnormal positive temperature dependence of the yield stress is a micro-cross slip model (Kear-Wilsdorf mechanism [17]) which is operative in well known $L1_2$ -type Ni_3Al

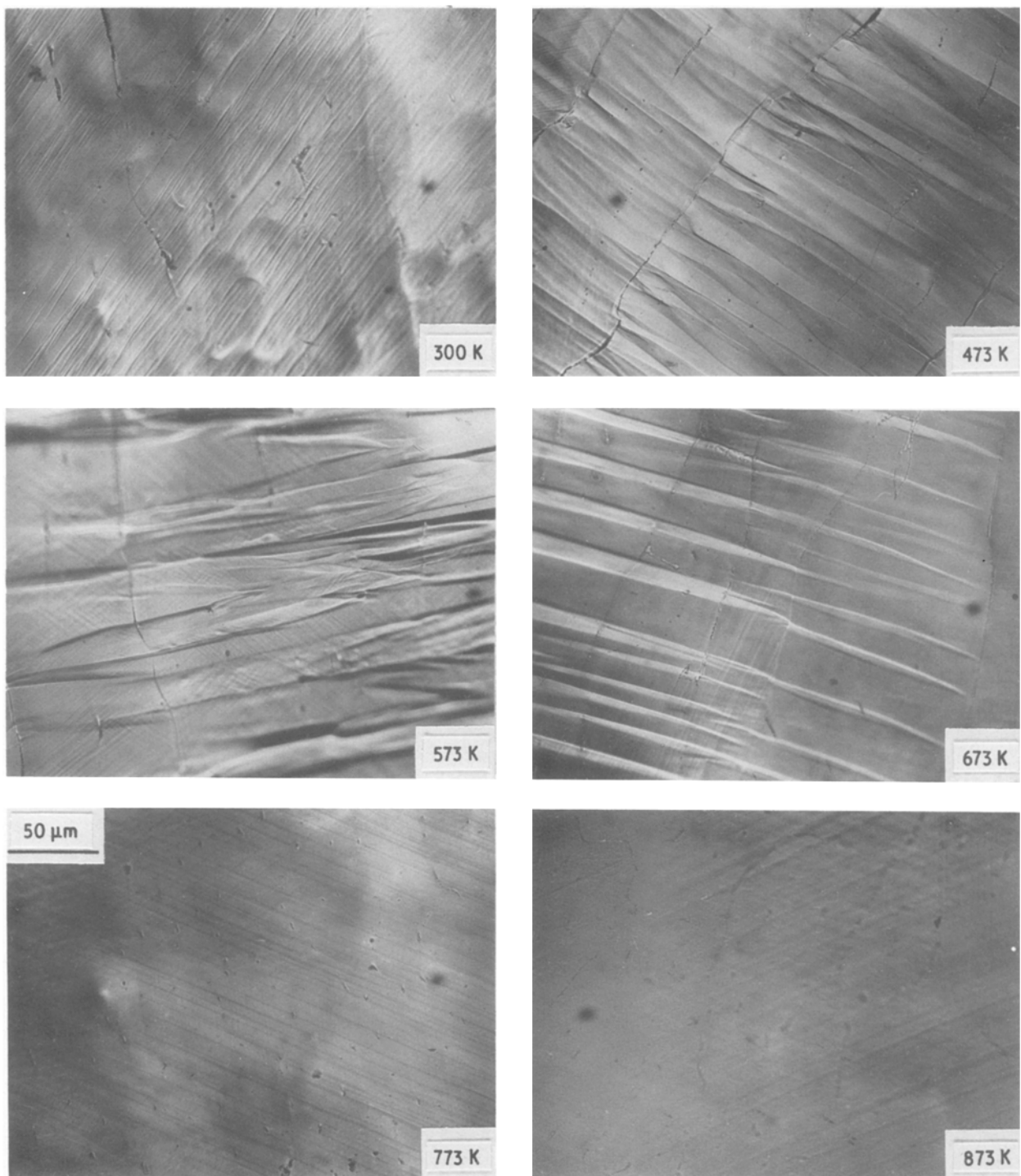


Figure 6 Deformation markings observed in CoTi polycrystals containing 49.5 at.% Ti and measured at a strain rate of $4.2 \times 10^{-4} \text{sec}^{-1}$. Note that the stress axes are shown approximately in the vertical axes of the photograph.

[18] and Co_3Ti [19]; it has been suggested that the increased stress occurs because of the thermally activated cross-slip of screw dislocations from glide plane to another plane, which thus become sessile and act as obstacles for further dislocation motion. The driving force for this cross-slip is the anisotropy of the anti-phase boundary (APB) energy on both planes. If the slip system in this temperature region is $\langle 111 \rangle$ type, this mechanism would be responsible because it is possible for the $\langle 111 \rangle$ type dislocation to decompose into two partials of $a/2\langle 111 \rangle$ with the APB fault. Indeed, as described in the previous sections, the slip system in B2-type compounds with high ordering

energy was usually operative on the $\langle 111 \rangle$ type direction at low temperature.

The second possible explanation may be attributed to the transition or the interaction between region (i) (low temperatures) and region (iii) (high temperatures). For example, the interaction between dislocations operating at both temperatures might produce an increased stress at this temperature. Otherwise, the positive temperature dependence simply appeared as the transition from region (i), at which deformation stress is inherently low, to region (ii) at which deformation stress is intrinsically high. The occurrence of kinks accompanied by serrations may

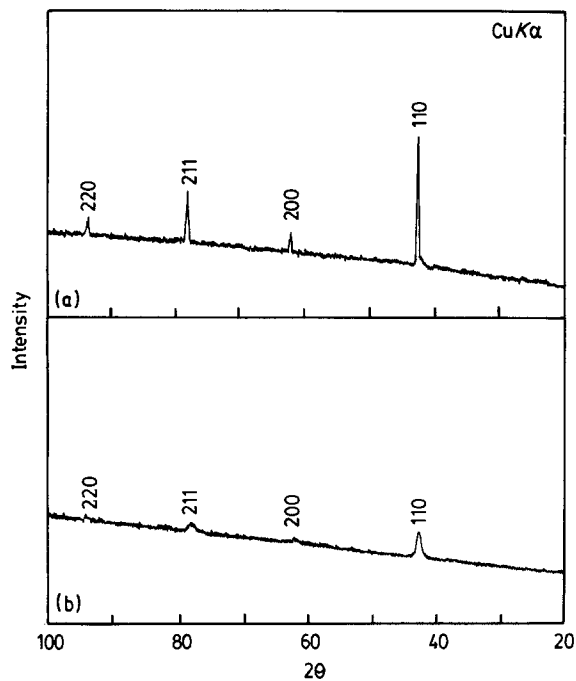


Figure 7 X-ray diffraction patterns of CoTi measured on (a) well-annealed and (b) as-crushed powders.

be a consequence of the flow stress drop which accommodates the rapid hardening or increased stress due to the slip deformation. In other words, it may be suggested that kinks were not the origin of the increased extra yield stresses, i.e. rapid strain-hardening rate.

The strong temperature-dependence of yield stress in region (iii) (high temperatures) of B2-type compound with high ordering energy has been generally interpreted by a mechanism similar to that in region (i) (low temperatures); the yield stress is controlled again by the Peierls double kink mechanism of the dislocations but they are of a different type to those appearing at low temperatures. It is widely accepted that the slip on the $\langle 001 \rangle$ direction is somewhat fundamental to the deformation of B2-type compounds at higher temperatures.

At all temperatures investigated, deviation from stoichiometry increased the yield stress. The major hardening effect may be a raising of the athermal temperature term in the yield stress, i.e. attributed to the strong solid solution hardening due to excess cobalt atoms. The peak temperature occurring on the transition from region (ii) to region (iii) also showed compositional dependence; deviation from stoichiometry produced a higher peak temperature. If this peak is due to the transition of the slip system (i.e. $\langle 111 \rangle$ slip to $\langle 100 \rangle$ slip), this compositional variation is consistent with that in FeAl observed by Mendiratta *et al.* [4].

The rate-controlling mechanism responsible for the deformation of the CoTi compound was thus considered based only on the polycrystalline materials. Therefore, extensive studies using CoTi single crystals should be made. The slip directions, as well as the slip planes, must be determined as a function of testing temperature, composition, strain rate and initial orientation of crystals. The ductile behaviour should also be evaluated.

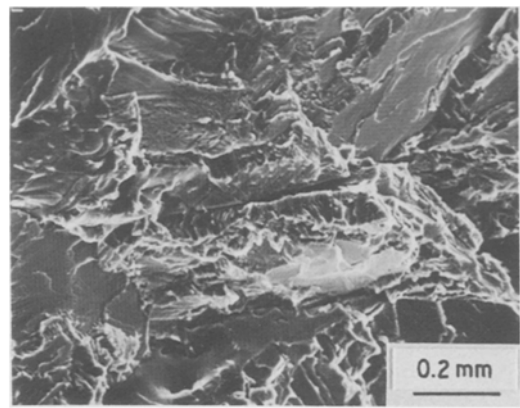


Figure 8 Fractography of CoTi polycrystals containing 50 at.% Ti which was fractured by bending at room temperature.

5. Conclusions

Compression tests using polycrystalline B2-type CoTi intermetallic compound were performed as a function of testing temperature, composition and strain rate. The results obtained are as follows.

1. Four distinct temperature regions were distinguished; a low temperature region where the yield stress rapidly decreased with temperature, an intermediate temperature region where the yield stress increased with temperature, a high temperature region where the yield stress again rapidly decreased with temperature, and finally very high temperature region where the yield stress slowly decreased with temperature.

2. Deviation of composition from stoichiometry resulted in increased yield stress values over whole temperature region.

3. Very high strain-hardening rate was investigated in the intermediate temperature region, accompanied by the load drop (i.e. serrations on the stress-strain curves) and audible clicks.

4. A clear positive strain-rate dependence of the yield stress was seen in the higher two temperature regions.

5. Slip traces were observed at all temperatures. However, in the intermediate temperature region, kinks were the major deformation mode mostly along a direction normal to the stress axis.

Acknowledgement

This work was supported in part by the Grant-In-Aid of Scientific Research from the Ministry of Education, Science and Culture under contract no. 61460203.

References

1. N. S. STOLLOF, "Strengthening Methods in Crystals", edited by A. Kelly (Elsevier, Essex, 1971) p. 193.
2. M. YAMAGUCHI and Y. UMAKOSHI, "Intermetallic Compounds" (Nikkan Kogyo, Tokyo, 1984) p. 48.
3. Y. UMAKOSHI and M. YAMAGUCHI, *Phil. Mag.* **41** (1980) 573.
4. M. D. MENDIRATTA, H.-M. KIM and H. A. LIPSITT, *Met. Trans. A* **15A** (1984) 395.
5. K. MURAKAMI, Y. UMAKOSHI and M. YAMAGUCHI, *Phil. Mag. A*: **37** (1978) 719.
6. M. YAMAGUCHI and Y. UMAKOSHI, *ibid.* **39A** (1979) 33.
7. J. L. MURRAY, *Bull. Alloy Phase Diagr.* **3** (1982) 74.

8. A. BALL, *Metal Sci. J.* **1** (1967) 47.
9. T. PASCOE and C. W. A. NEWY, *Phys. Status Solidi* **29** (1968) 357.
10. T. TAKASUGI and O. IZUMI, *Phys. Status Solidi (a)* **102** (1987) 699.
11. R. J. WASILEWSKI, S. R. BUTLER and J. E. HANLON, *Trans. Met. Soc. AIME* **239** (1967) 1357.
12. R. T. PASCOE and C. W. A. NEWY, *Metal Sci. J.* **2** (1968) 138.
13. D. L. WOOD and J. H. WESTBROOK, *Trans. Met. Soc. AIME* **224** (1962) 1024.
14. A. R. CAUSEY and E. TEGHTSOONIAN, *Met. Trans.* **1** (1970) 1177.
15. A. K. MUKHERJEE and J. E. DORN, *Trans. Met. Soc. AIME* **230** (1964) 1065.
16. E. M. SCHULSON and E. TEGHTSOONIAN, *Phil. Mag.* **19** (1969) 155.
17. B. H. KEAR and H. G. F. WILSDORF, *Trans. Met. Soc. AIME* **224** (1962) 382.
18. D. P. POPE and S. S. EZZ, *Int. Natl. Rev.* **29** (1984) 136.
19. T. TAKASUGI, S. HIRAKAWA, O. IZUMI, S. ONO and S. WATANABE, *Acta Metall.* **35** (1987) 2015.

*Received 2 April
and accepted 16 June 1987*